Renormalization group reduction of pulse dynamics in thermally loaded optical parametric oscillators

Richard O. Moore[(1)], **Keith Promislow**[(2)]

[(1)] Department of Mathematical Sciences

New Jersey Institute of Technology

323 Martin Luther King, Jr. Blvd., Newark, NJ 07102

[(2)] Department of Mathematics

Michigan State University

East Lansing, MI 48824

CAMS Report 0506-34, Spring 2006

Center for Applied Mathematics and Statistics

NJIT

Renormalization group reduction of pulse dynamics in thermally loaded optical parametric oscillators

Richard O. Moore[†], **Keith Promislow**[‡]

† Department of Mathematical Sciences, New Jersey Institute of Technology
323 Martin Luther King, Jr. Blvd., University Heights, Newark, NJ 07102
tel: (973)596-5557, fax: (973)596-5591, e-mail: richard.o.moore@njit.edu
‡ Department of Mathematics, Michigan State University, East Lansing, MI 48824

Abstract. We derive a perturbed parametrically forced nonlinear Schrödinger equation to model pulse evolution in an optical parametric oscillator with absorption-induced heating. We apply both a rigorous renormalization group technique and the formal Wilsonian renormalization group to obtain a low-dimensional system of equations which captures the mutual interaction of pulses as well as their response to the thermally induced potential. We compare the methodologies of the two approaches and find that the two reduced systems agree to leading order, and compare well to simulations of the full equation, predicting the formation of stably bound pulse pairs.

PACS number: 02.30.Jr Partial differential equations, 04.30.Nk Wave propagation and interactions

1. Introduction

Optical parametric processes are the subject of much current interest in the optical community for their potential use in a variety of applications, including communications, infrared spectroscopy, medical diagnosis, and military countermeasures [11, 16, 24]. The partial differential equations (PDEs) that model these processes, typically envelope equations derived from Maxwell's relations, redistribute energy through both nonlinearity and dispersion. In many cases of interest, nonlinearity and dispersion balance each other to produce localized steady and quasi-steady states, suggesting operating parameters for the robust generation of optical pulses or laser beams, for example. Determining the stability and slow dynamics of these pulses, particularly under the influence of external perturbations, presents a difficult and important problem.

Recently, several authors [8,12,19,22] have developed techniques to reduce the pulse dynamics in a wide class of nonlinear dispersive PDEs to finite-dimensional systems of ordinary differential equations (ODEs). Within the scope of these methods, a flow

$$U_t = F(U) \tag{1}$$

given by an operator F, which possesses quasi-steady states $\Phi(\mathbf{p})$ that are parameterized by $\mathbf{p} \in \mathbf{R}^N$, can be reduced to the flow of $\mathbf{p}(t)$ and a small remainder $W(t)$. The infinite-dimensional flow of U is reduced to the evolution of a finite collection of parameters (coordinates), producing a system that is more amenable to analysis and more efficient to solve numerically. Whereas formal collective coordinate reductions are often only heuristically justified (see Ref. 21 and references therein), the approach developed in Ref. 19 borrows from renormalization group (RG) theory to develop estimates that show the remainder W stays small throughout the evolution. A key step in obtaining such bounds is to break the temporal dynamics into a sequence of initial-value problems (IVPs), each dominated by a fixed-in-time linear operator. The finite-dimensional $\mathbf{p}$-state is renormalized at the start of each time segment, removing secularity from the remainder W to prevent its growth. The solution U is attracted into a neighborhood of the manifold parameterized by $\mathbf{p}$, and the salient dynamics are thus obtained as a family of ODEs. We compare this rigorous approach with the formal Wilsonian-style RG showing that the two arrive, to leading order, at equivalent reduced flows for the problem under consideration.

Various RG approaches to studying the low-dimensional dynamics of PDEs have been applied to diffusive equations such as the Brusselator, Ginzburg-Landau, Fisher-Kolmogorov-Petrovsky-Piskunov and Korteweg-de Vries equations [8,12], and to dissipative-diffusive equations such as the Newell-Whitehead equation [9]. The rigorous RG approach presented here has been applied previously to the stability of fronts and of pulse trains in the parametrically forced nonlinear Schrödinger (PNLS) equation, a dissipative-dispersive equation. The novelty of the application considered here lies in the coupling of the dynamics of the optical pulses, which reside on a fast spatial scale, to the variations induced by the thermal profile, which lives on a slow spatial scale. The rigorous quantification of this coupling between the evolution of the pulse positions, amplitudes, and widths and the slow spatial variation of the thermal profile requires an application of the ideas of Ref. [23] addressing the preservation of exponential dichotomies in the presence of slowly varying parameters within the linear operator. This affords a substantial extension of the applicability of the RG methodology. The combination of tail-tail and pulse-background interactions leads to several interesting results, including velocities which are algebraically rather than exponentially small, the first rigorous prediction of bound two-pulses from the reduced RG form of the PNLS equation, and the prediction of $O(1)$ changes in the shape of an evolving pulse.

This paper is organized as follows. In Sec. 2 we derive the perturbed PNLS equation as a reduction of a coupled system of envelope equations. We review the nature of the linearization about a single pulse solution for the unperturbed equation, and introduce a fixed refractive index perturbation. In Sec. 3 we apply the rigorous RG method to obtain our main result presented in Theorem 1, i.e., a reduced family of equations for pulse position evolution, and we compare the derivation to that of the formal Wilsonian RG method. In Sec. 4 we analyze the reduced equations and present criteria for the formation of stable pulse pairs in Theorem 2. Finally, we compare the reduced equations

to numerical simulations of the PNLS equation.

2. The PNLS equation

An OPO is a frequency-conversion device that provides high-powered, highly coherent, directional light at frequencies that are not readily available through material resonances used in conventional lasers. It is based on the parametric gain provided by a nonlinear medium such as a quadratic crystal (e.g., $LiNbO_3$ [25] or KTP [2]), and is otherwise similar to a laser in that the gain medium is situated inside of a cavity that is resonant at one or more of the frequencies of light present. In the case of a quadratic medium, the nonlinearity selects these frequencies in resonant triads, called *pump*, *signal* and *idler* frequencies, when the OPO is configured for nondegenerate operation, or in resonant pairs when the OPO is configured for degenerate operation, in which the idler and signal frequencies are equal. A schematic diagram of a nondegenerate OPO is given in Fig. 1. In addition to having a nonlinear polarization response, the gain medium is generally linearly dispersive and has a significant coefficient of absorption. Absorption of optical energy can have a profound effect on the OPO's behavior [18], particularly considering the sensitive dependence of linear field evolution on the refractive index, and the dependence of refractive index on temperature [14].

2.1. Derivation of the PNLS equation

We model the impact of absorption of optical energy on a degenerate OPO by imposing a nonuniform refractive index on the crystal and analyzing the interaction between beams making a single pass through the device. This effectively reduces the OPO to what is called an optical parametric amplifier (OPA). The coupled envelope equations for the electric fields propagating through the OPA (along coordinate z) at the two resonant frequencies can be derived from Maxwell's equations as [17]

$$\frac{\partial E_p}{\partial z} - \frac{i}{2k_p}\nabla_\perp^2 E_p - \frac{2\pi i}{\lambda_p}\Delta n_p E_p + \frac{\alpha_p}{2}E_p = \frac{\pi i d}{n_p \lambda_p}E_s^2 e^{-i\Delta k z} + S(z, x_\perp), \tag{2}$$

$$\frac{\partial E_s}{\partial z} - \frac{i}{2k_s}\nabla_\perp^2 E_s - \frac{2\pi i}{\lambda_s}\Delta n_s E_s + \frac{\alpha_s}{2}E_s = \frac{\pi i d}{n_s \lambda_s}E_p E_s^* e^{i\Delta k z}, \tag{3}$$

where the E_j are the electric field amplitudes at the optical frequencies in resonance, the pump frequency ω_p and the signal frequency ω_s. The Laplacian $\nabla_\perp^2$ describes diffraction (or dispersion) in the plane orthogonal to the direction of propagation. The symbols k_j, λ_j, n_j, and α_j denote, respectively, the propagation constants, free-space wavelengths, ambient-temperature refractive indices, and absorption coefficients. The phase mismatch, $\Delta k = k_p - 2k_s$, reflects the dispersion in the medium, and the inhomogeneous term S is a distributed forcing term at the pump frequency ω_p. The nonlinear coefficient d is the material's effective quadratic response to waves interacting at the pump and signal polarizations. Finally, the perturbed refractive index terms, Δn_p and Δn_s, arise from heating of the material; their magnitudes can be calculated from

the temperature-dependent Sellmeier relations for lithium niobate [14], for example. We focus on perturbations Δn_s to the index at the signal wavelength, neglecting the perturbations Δn_p at the pump wavelength as a lower-order effect.

We assume that the linear component of Eqn. 2 is dominated by a large, negative phase mismatch ($k_p(-\Delta k) \gg 1/r_p^2$, where r_p is the characteristic pump beam radius), and that the pumping term is also large and of the form $S(z, x_\perp) = -i\bar{S}\exp(-i\Delta k z)$ with $\bar{S}$ real and positive. This, along with suitably scaled initial conditions on the pump and signal fields (see Ref. 20), enables us to substitute

$$\frac{\partial E_p}{\partial z} \to -i\Delta k E_p, \tag{4}$$

allowing us to slave the pump field to the signal field, i.e.,

$$E_p \approx \frac{1}{-\Delta k}\left(\frac{\pi d}{n_p \lambda_p} E_s^2 - \bar{S}\right) e^{-i\Delta k z}. \tag{5}$$

For simplicity we consider only a single, infinite transverse dimension, and substitute Eqn. 5 into Eqn. 3 with the following nondimensionalizations:

$$z = \frac{2}{\alpha_s} t, \qquad r_\perp = \sqrt{\frac{2}{\alpha_s k_s}}\, x, \quad \text{and} \quad E_s(r_\perp, z) = \sqrt{\frac{-\Delta k \alpha_s n_s n_p \lambda_s \lambda_p}{2\pi^2 d^2}}\, v(x,t), \tag{6}$$

resulting in the PNLS equation for the signal field in the large pump detuning regime,

$$i v_t + \frac{1}{2} v_{xx} + |v|^2 v + [i - a(x)]v - \gamma v^* = 0. \tag{7}$$

The dimensionless parameters γ and $a(x)$ are defined by

$$\gamma = \frac{2\pi \bar{S}}{\alpha_s n_s \lambda_s |\Delta k|} \qquad \text{and} \qquad a(x) = \frac{-4\pi}{\alpha_s \lambda_s} \Delta n(r_\perp).$$

The change of notation from z to t is to emphasize that the PNLS equation should be regarded as an initial-value problem.

Our study is motivated by a refractive index perturbation Δn arising from self-induced heating; however, there are several potential sources for such a perturbation, including imperfections in the nonlinear crystal, spatial deformation, and externally applied electric fields. These can potentially lead to a number of deleterious effects, including (thermal) lensing, detuning, and distortion of the linear modes, and they can change significantly the interaction between fields at different frequencies or in different spatial modes in the OPA [18]. We consider the simpler Eqn. 7 to study some of these effects in a more rigorous context than is possible in the full system presented by Eqns. 2 and 3. Equation 7 has been considered from a physical perspective by a number of authors [1, 3–6].

2.2. Pulse solutions and associated linearized operators

The PNLS equation has two soliton-like solutions over the range $1 \leq \gamma \leq \sqrt{1+a^2}$, as depicted in Fig. 2. The lower branch is always unstable, with nearby data lying in the basin of attraction either of the trivial solution or of the upper branch. The upper branch is stable for suitably small γ, but loses stability either through a Hopf bifurcation or via an essential instability as γ increases, as discussed below. We are interested in the dynamics of otherwise stable solitons, so we restrict our analysis to the stable portion of the upper solution branch.

To facilitate a study of the upper solution branch, we make a coordinate transformation that poses the PNLS Eqn. 7 in the form of Eqn. 1,

$$v = u(x)e^{i\theta} \quad \text{with} \quad \gamma e^{-2i\theta} = \sqrt{\gamma^2 - 1} + i. \tag{8}$$

Letting $U = (\Re(u), \Im(u))^T$ then gives

$$U_t = \begin{pmatrix} 0 & -\frac{1}{2}\partial_x^2 - \|U\|^2 + \eta_- \\ \frac{1}{2}\partial_x^2 + \|U\|^2 - \eta_+ & -2 \end{pmatrix} U, \tag{9}$$

where $\eta_\pm = a \pm \sqrt{\gamma^2 - 1}$.

The steady state solution on the upper branch is

$$\Phi = \begin{pmatrix} \phi(x - X) \\ 0 \end{pmatrix}, \tag{10}$$

with $\phi(s) = \sqrt{2\eta_+}\ \mathrm{sech}\,(\sqrt{2\eta_+}\ s)$. The arbitrary position X reflects the translation invariance in the PNLS Eqn. 7. Linearizing about this state gives $V_t = LV$ with

$$L \equiv \begin{pmatrix} 0 & D \\ -C & -2 \end{pmatrix} \quad \text{and adjoint} \quad L^\dagger = \begin{pmatrix} 0 & -C \\ D & -2 \end{pmatrix}, \tag{11}$$

where

$$D \equiv -\left(\frac{1}{2}\partial_x^2 + \phi^2 - \eta_-\right) \quad \text{and} \quad C \equiv -\left(\frac{1}{2}\partial_x^2 + 3\phi^2 - \eta_+\right). \tag{12}$$

We give a brief summary of results obtained previously [3, 7, 20] for the PNLS equation when a is constant. The point and essential spectrum of the stable steady state inherit structure from the symmetries inherent in Eqn. 7. The spectrum is doubly reflection-symmetric about (-1,0) [7], so that we need only consider a single quadrant of the eigenvalue plane. On both branches, translation invariance produces a single eigenvalue λ_t at the origin provided $\gamma > 1$; if $\gamma = 1$, this eigenvalue has multiplicity 2. The degeneracy arises from a hidden symmetry upon the merging of the two solution branches at $\gamma = 1$ (see Fig. 2), as they limit to a neutrally stable solution. The second eigenfunction associated with the zero eigenvalue λ_p is the instantaneous variation of the solution with respect to γ at the turning point. When $\gamma > \sqrt{1+a^2}$ the lower branch

ceases to exist and the essential spectrum crosses the imaginary axis, driving the upper branch unstable.

Numerical evaluation of the Evans function [7] shows that as γ increases from 1, a third discrete eigenvalue λ_q bifurcates out of the essential spectrum and approaches the origin (at first proceeding down the symmetry abscissa $-1+iy$ if $a > 1$). This eigenvalue eventually collides with λ_p to form a complex conjugate pair of eigenvalues that lift off of the real axis. These ultimately cross the imaginary axis in a Hopf bifurcation after (before) the occurrence of the essential instability described above if $a < a_{\rm crit} \approx 2.645$ ($a > a_{\rm crit}$). To avoid the essential and Hopf instabilities, we consider only ranges of a that lie within the patterned region depicted in Fig. 3.

It is of some interest to relate this spectral picture to the perturbative limit of the nonlinear Schrödinger (NLS) equation studied in Ref. 15. Figure 2 of that reference corresponds to the case where $a > 1.132$ (i.e., a is sufficiently large so that λ_p and its reflection-symmetric counterpart $\bar{\lambda}_p$ collide at $(-1, 0)$ before colliding again with λ_q on the symmetry abscissa) and $1 < \gamma_1 < \gamma < \gamma_2$, where γ_1 is the value of γ at which λ_p collides with $\bar{\lambda}_p$ and γ_2 is the value of γ at which the resulting eigenvalue collides with λ_q on the symmetry abscissa. Figure 4 illustrates this progression. Straightforward calculations show that $\lambda_t = 0$ and its symmetric counterpart at $\bar{\lambda}_t = -2$ are related to the odd eigenfunctions of the NLS linearization; i.e., they relate to the translation and Galilean invariances in the original NLS equation (the first of which persists in the PNLS equation). The other two eigenvalues that emerge from the origin as one moves away from the NLS limit are associated with the broken scale and rotational invariances.

We consider the case $\gamma - 1 = \mathcal{O}(1)$, in which the sole eigenfunction driving the dynamics is that associated with translational invariance, i.e.,

$$\Psi = \begin{pmatrix} \phi'(x - X) \\ 0 \end{pmatrix} \quad \text{and} \quad \Psi^\dagger = \frac{1}{\Theta} \begin{pmatrix} 2D^{-1}\phi'(x - X) \\ \phi'(x - X) \end{pmatrix}, \tag{13}$$

where the bi-orthogonal eigenfunction pair has been normalized to give $\langle \Psi, \Psi^\dagger \rangle = 1$ by choosing

$$\Theta = 2 \int \phi' D^{-1} \phi' \, dx. \tag{14}$$

The operator D is positive except for a single negative eigenfunction, ϕ. Since ϕ' has zero projection against ϕ it follows that $\Theta \geq \Theta_0$ for some $\Theta_0 > 0$; see Lemma 3.2 of Ref. 20.

2.3. Refractive index perturbation

In Ref. 18, the self-induced heating of the OPA via the absorption of optical energy into the nonlinear crystal is incorporated by coupling a diffusion equation to Eqns. 2 and 3 through a refractive index perturbation that is nonuniform in the transverse dimension as well as in the longitudinal (propagation) dimension. To simplify our

model, we consider a fixed, slowly varying transverse profile $a(\epsilon x)$, with $0 < \epsilon \ll 1$. A Gaussian profile for $a(\epsilon x)$ is a reasonable approximation to the equilibrium temperature distribution driven by a beam-shaped forcing term:

$$a(\epsilon x) = a_0 + a_1 e^{-(\epsilon x)^2/2}. \tag{15}$$

We emphasize that while the variation in a is slow, the total variation, given by a_1, is $\mathcal{O}(1)$. This leads to the object of our investigation, a modified form of Eqn. 9

$$U_t = \begin{pmatrix} 0 & -\frac{1}{2}\partial_x^2 - \|U\|^2 + \eta_-(x) \\ \frac{1}{2}\partial_x^2 + \|U\|^2 - \eta_+(x) & -2 \end{pmatrix} U, \tag{16}$$

where $\eta_\pm(x) = a(\epsilon x) \pm \sqrt{\gamma^2 - 1}$. Following the notation of Eq. 1, we will denote the right-hand side of Eq. 16 by $F(U)$.

3. The N-pulse ansatz and reduced dynamics

To obtain a finite-dimensional dynamical system that captures the effect of a nonuniform refractive index on quasi-steady states of the perturbed PNLS Eqn. 16, we project the flow of U onto a manifold of N-pulses. The manifold is parameterized by the pulse positions, which serve as collective coordinates for the reduced equations. Under suitable assumptions, this case falls within the scope of applications treated generally in Ref. 19. Rather than reiterate the discussion contained therein, we present the hypotheses H0 through H4 and discuss their relevance to the derivation of our main result, Theorem 1.

3.1. Rigorous renormalization

We introduce an ansatz consisting of a collection of well-separated quasi-steady pulses. Each pulse has its shape determined by the local value of the refractive index:

$$\Phi(x; X) = \begin{pmatrix} \phi_X(x - X) \\ 0 \end{pmatrix} \quad \text{with} \tag{17}$$

$$\phi_X(s) = \sqrt{2\eta_X}\,\mathrm{sech}\left(\sqrt{2\eta_X}\,s\right), \tag{18}$$

where for notational simplicity we introduce $\eta_X \equiv \eta_+(X)$. The ansatz for a sequence of N pulses is

$$\Phi_N(x; \vec{X}) = \sum_{j=1}^{N} \alpha_j \Phi_j\left(x - X_j\right), \tag{19}$$

where $\vec{X} = (X_1, \ldots, X_N)$, $\Phi_j = \Phi(x; X_j)$, and each α_j assumes the value $+1$ or -1. Any solution of Eqn. 16 can be decomposed as

$$U(x,t) = \Phi_N + W(x,t), \tag{20}$$

where W is the remainder term. We insert the decomposition into Eq. 16 and expand in orders of W,

$$\nabla_{\vec{X}}\Phi_n \cdot \frac{d\vec{X}}{dt} + W_t = F(\Phi_N + W) = F(\Phi_N) + L_{\vec{X}}W + \mathcal{N}(W), \tag{21}$$

where $L_{\vec{X}}$ is the linearization about $\Phi_N(\cdot, \vec{X})$ and $\mathcal{N}$ denotes the terms nonlinear in W.

The linearization $L_{\vec{X}}$ of Eqn. 16 about Φ_N is given by

$$L_{\vec{X}} \equiv \begin{pmatrix} 0 & D_{\vec{X}} \\ -C_{\vec{X}} & -2 \end{pmatrix} \tag{22}$$

where

$$D_{\vec{X}} \equiv -\left(\frac{1}{2}\partial_x^2 - \eta_-(x) + \sum_{i=1}^{N}\phi_i^2 + 2\mathcal{V}\right), \tag{23}$$

$$C_{\vec{X}} \equiv -\left(\frac{1}{2}\partial_x^2 - \eta_+(x) + 3\sum_{i=1}^{N}\phi_i^2 + 6\mathcal{V}\right), \tag{24}$$

and

$$\mathcal{V} = \sum_{\substack{i,j=1 \\ i\neq j}}^{N} \alpha_i\alpha_j\phi_i\phi_j \tag{25}$$

represents small cross terms. We emphasize that $\phi_i = \phi_{X_i}(x - X_i)$, takes its scaling from its location X_i.

The decomposition and associated evolution given by Eqns. 20 and 21 are not unique; the goal is to determine an evolution for the pulse positions $\vec{X}(t)$ which forces the remainder W to decay. For a given pulse configuration $\vec{X}$, we define the minimum pulse separation $\Delta X = \min\{|X_i - X_j| \Big| i \neq j\}$, and verify the hypotheses below for $\vec{X} \in \mathcal{K} = \{\vec{X} \Big| \Delta X \geq l_s\}$, deducing our main result, contained in Theorem 1, from Theorem 1 of Ref. 19. We consider the regime in which the pulse-pulse interaction is comparable to the influence of the refractive index, taking l_s large enough that $\delta \equiv e^{-\sqrt{2\eta_0}\Delta X}$, with $\eta_0 = \eta_+|_{X=0}$, satisfies $\delta = \mathcal{O}(\epsilon^2)$ for all $\vec{X} \in \mathcal{K}$.

H0: Quasi-stationarity. The ansatz Φ_N represents quasi-steady states in the sense that

$$\|F(\Phi_N(\cdot, \vec{X}))\|_{H^1} \leq c\epsilon^2. \tag{26}$$

Proof: For the case $N = 2$, the quantity $F(\Phi_N) = \epsilon^2 G_{t_0}$ where G_{t_0} is given by Eqn. 56. It is straightforward to verify (26) for $\vec{X} \in \mathcal{K}$. Generalizations to $N > 2$ are merely concatenations of the result for $N = 2$.

H1: Normal hyperbolicity. The spectrum of each linearized operator $L_{\vec{X}}$ may be decomposed into a stable part σ_s, strictly contained in the left-half complex plane, and a slow part σ_0, comprised of a fixed, finite number of small eigenvalues. Specifically,

$$\sigma(L_{\vec{X}}) = \sigma_s \cup \sigma_0, \tag{27}$$

where $\sigma_s \subset \{\lambda \big| \operatorname{Re}\lambda \leq -k\}$ for some $k > 0$, and $\sigma_0 \subset \{\lambda \big| |\lambda| \leq c\epsilon^2\}$ and consists of N eigenvalues, up to multiplicity. Both N and k may be chosen independently of $\vec{X} \in \mathcal{K}$.

Proof: The preservation of exponential dichotomies for systems with slowly varying coefficients (see Ref. 13 and Appendix A.2 of Ref. 23), guarantees that the stable (unstable) manifold at $+\infty$ ($-\infty$) associated with the first order system, $L_{\vec{X}}W = 0$, depends smoothly upon the slow length scale ϵ as $\epsilon \to \infty$. In particular, from the usual Evans function construction [15] we deduce the smooth dependence of the eigenfunctions of $L_{\vec{X}}$ and its adjoint upon the parameters $\vec{X}$. For the regime of interest to us, where $\exp(-\sqrt{2\overline{\eta}}\Delta X)$ and ϵ^2 are of the same order, we are justified in considering a perturbation expansion of the eigenpairs.

We are particularly concerned with the leading-order behavior of the eigenpairs of $L_{\vec{X}}$ that perturb off of the degenerate translational eigenvalue at infinite pulse separation. The details are complicated by the fact that the refractive index perturbation introduces $\mathcal{O}(\epsilon^2)$ terms to $L_{\vec{X}}$ both directly, by perturbing the operator, and indirectly, by changing the asymptotic quasi-steady states.

We proceed by first finding the correct splitting of the $\mathcal{O}(1)$ eigenfunctions, and then finding the $\mathcal{O}(\epsilon^2)$ corrections to the eigenvalues. As the splitting of the asymptotic eigenfunctions is dictated by the two-pulse interaction, we include the refractive index perturbation only in the second step. We set

$$L_{00} = \begin{pmatrix} 0 & D_{00} \\ -C_{00} & -2 \end{pmatrix}, \tag{28}$$

where

$$D_{00} = -\left(\frac{1}{2}\partial_x^2 + 2\eta_+\left[\operatorname{sech}^2\left(\sqrt{2\eta_+}(x-X_1)\right) + \operatorname{sech}^2\left(\sqrt{2\eta_+}(x-X_2)\right)\right] - \eta_-\right) \tag{29}$$

and

$$C_{00} = -\left(\frac{1}{2}\partial_x^2 + 6\eta_+\left[\operatorname{sech}^2\left(\sqrt{2\eta_+}(x-X_1)\right) + \operatorname{sech}^2\left(\sqrt{2\eta_+}(x-X_2)\right)\right] - \eta_+\right), \tag{30}$$

and we assume without loss of generality that $X_2 > X_1$. The asymptotic spectrum of L_{00} as $X_2 - X_1 \to \infty$ has a zero eigenvalue of algebraic multiplicity 2 associated with the asymptotic zero eigenfunctions of C_{00}. From Ref. 23 we know that the exponential dichotomy of the eigenvalue problem persists under the slow spatial variation of the

potentials η_+ and η_- and that, as $X_2 - X_1$ assumes a finite value, the new eigenfunctions split as linear combinations of the asymptotic eigenfunctions to leading order, so that

$$\Psi_+ = \sigma_+^{(1)}\Psi_1 + \sigma_+^{(2)}\Psi_2, \tag{31}$$

$$\Psi_- = \sigma_-^{(1)}\Psi_1 + \sigma_-^{(2)}\Psi_2. \tag{32}$$

The eigenvalue equations then take the form

$$L_{00}\Psi_\pm^{(0)} + L_\Delta \Psi_\pm^{(0)} = \lambda_\pm \Psi_\pm^{(0)}, \tag{33}$$

with each term of $\mathcal{O}(\epsilon^2 + \exp[-\sqrt{2\eta_+}\Delta X])$. The operator L_Δ includes the effect of the perturbed refractive index and its impact on the steady states Ψ_1 and Ψ_2.

Taking the inner product of this expression with the asymptotic eigenfunctions of $L_{00}^\dagger$ provides a symmetric matrix whose eigenvectors are the allowed values of σ_+ and σ_-:

$$\begin{pmatrix} \frac{1}{2}\epsilon^2 a_1\sqrt{2\eta_+}\left(\frac{\pi^2}{18}+\frac{2}{3}\right) & -4(2\eta_+)^{5/2}e^{-\sqrt{2\eta_+}\Delta X} \\ -4(2\eta_+)^{5/2}e^{-\sqrt{2\eta_+}\Delta X} & \frac{1}{2}\epsilon^2 a_1\sqrt{2\eta_+}\left(\frac{\pi^2}{18}+\frac{2}{3}\right) \end{pmatrix} \begin{pmatrix} \sigma_\pm^{(1)} \\ \sigma_\pm^{(2)} \end{pmatrix} = \lambda_\pm \Theta_0 \begin{pmatrix} \sigma_\pm^{(1)} \\ \sigma_\pm^{(2)} \end{pmatrix}. \tag{34}$$

This provides the leading order terms of the eigenpairs:

$$\Psi_\pm^{(0)} = \Psi_1^{(0)} \pm \Psi_2^{(0)} \quad \text{with} \tag{35}$$

$$\lambda_\pm = \frac{1}{\Theta_0}\left[\frac{1}{2}\epsilon^2 a_1\sqrt{2\eta_+}\left(\frac{\pi^2}{18}+\frac{2}{3}\right) \mp 4(2\eta_+)^{5/2}\exp(-\sqrt{2\eta_+}\Delta X)\right]. \tag{36}$$

H2: Semigroup property. Each fixed operator $L_{\vec{X}}$ generates a $\mathcal{C}_0$ semigroup $S_{\vec{X}}$ which satisfies

$$\|S_{\vec{X}}(t)u\|_{H^1} \leq Me^{-kt}\|u\|_{H^1} \quad \text{for all } t \geq 0, u \in \mathcal{X}_{\vec{X}}, \tag{37}$$

where $\mathcal{X}_{\vec{X}}$ is the $L_{\vec{X}}$ invariant subspace of H^1 of codimension N associated with the spectrum σ_s. Moreover, M may be chosen independent of $\vec{X} \in \mathcal{K}$.

Proof: This is a consequence of Proposition 4.1 of Ref. 20.

H3: Compatibility. The slow space $\mathcal{Y}_{\vec{X}}$, the spectral complement of $\mathcal{X}_{\vec{X}}$, is well-approximated by the tangent plane of the graph of the ansatz, $\Phi_N(\cdot, \vec{X})$. That is, there is a constant $\delta_C > 0$ small enough and a given ordering $\{\Psi_1, \ldots, \Psi_N\}$ of the eigenfunctions spanning $\mathcal{Y}_{\vec{X}}$ such that

$$\left\| \Psi_i(\vec{X}) - \frac{\partial \Phi_N(\cdot, \vec{X})}{\partial X_i} \right\|_{H^1} \leq \delta_C \qquad \text{for } i = 1, \ldots, N \tag{38}$$

for each point $\vec{X} \in \mathcal{K}$. Here $\delta_C > 0$ is independent of $\vec{X} \in \mathcal{K}$.

Proof: For the case $N = 2$ we see from Eqn. 35 that the eigenfunctions Ψ_1 and Ψ_2 form a basis for $\mathcal{Y}_{\vec{X}}$, up to $\mathcal{O}(\epsilon^2)$. This verifies Eqn. 38 with $\delta_C = \epsilon^2$, which we can take as small as is necessary. In fact, defining the $N \times N$ matrix M with entries given by

$$M_{ij} = \left(\frac{\partial \Phi_N(\cdot, \vec{X})}{\partial X_i}, \Psi_j^\dagger(\vec{X}) \right)_2, \tag{39}$$

we observe that Eqn. 38 implies

$$M = I_{N\times N} + \mathcal{O}(\delta_C), \tag{40}$$

and we merely need δ_C so small as to make M invertible.

H4: Stability. The adjoint eigenvectors normalized so that $(\Psi_i, \Psi_j^\dagger)_2 = \delta_{ij}$, where δ_{ij} is the Kronecker delta, are uniformly bounded and depend smoothly upon $\vec{X}$ for all $\vec{X} \in \mathcal{K}$.

Proof: That Ψ_i and $\Psi_i^\dagger$ may be taken to depend smoothly upon $\vec{X}$ follows from Ref. 23. That they are smooth under the normalization requires, in the case $N = 1$, that the inner product Θ defined in Eqn. 14 is bounded away from zero, as previously observed. If $N = 2$, it is clear from Eqn. 35 that $(\Psi_\pm, \Psi_\pm^\dagger) = 2\Theta + \mathcal{O}(\epsilon^2) > 0$. Similar results hold for $N > 2$.

Having verified the hypotheses (H0-H4), we give a sketch of the renormalization procedure which leads to the main result, stated in Theorem 1 below. Given initial data U_0 close to the manifold $\mathcal{M} = \left\{ \Phi_N(\cdot, \vec{X}) \middle| \vec{X} \in \mathcal{K} \right\}$ of quasi-steady solutions, we choose an initial configuration, $\vec{X}_0$, for the pulses by demanding that

$$W_0 \equiv U_0 - \Phi_N(\cdot, \vec{X}_0) \in \mathcal{X}_{\vec{X}_0}. \tag{41}$$

This is a system of N equations for $\vec{X}_0$ which has a unique solution given (H3), (H4), and $\mathrm{dist}(U_0, \mathcal{M})$ sufficiently small. The choice of $\vec{X}_0$ also fixes the decaying space $\mathcal{Y}_{\vec{X}_0}$. The linearized operator $L_{\vec{X}(t)}$ appearing in Eq. 21 is time-dependent; however, we may decompose it into constant-coefficient and secular parts,

$$L_{\vec{X}(t)} = L_{\vec{X}_0} + \overbrace{L_{\vec{X}} - L_{\vec{X}_0}}^{\mathcal{S}(t_0,t)}, \tag{42}$$

rewriting Eq. 21 as

$$\nabla_{\vec{X}} \Phi_n \cdot \frac{d\vec{X}}{dt} + W_t = F(\Phi_N) + L_{\vec{X}_0} W + \mathcal{N}(W) + \mathcal{S}(t_0, t) W. \tag{43}$$

We further demand that W remains in the decaying space $\mathcal{Y}_{\vec{X}_0}$ of $L_{\vec{X}_0}$, by imposing the condition

$$P_{\vec{X}_0} W(\cdot, t) = 0, \tag{44}$$

where $P_{\vec{X}_0}$ is the $L_{\vec{X}_0}$ spectral projection onto the N-dimensional space $\mathcal{X}_{\vec{X}_0}$. These N conditions remove all degeneracy from the decomposition, Eqn. 20, and determine the pulse velocities via the equivalent system contained in Eq. 49. Under the conditions given by Eqns. 41 and 44, the remainder W evolves according to

$$W_t = L_{\vec{X}_0} W + Q_{\vec{X}_0} \left\{ \mathcal{N}(W) + \mathcal{S}(t_0, t)W + F(\Phi_N) - \nabla_{\vec{X}} \Phi_N \cdot \frac{d\vec{X}}{dt} \right\} \tag{45}$$

and

$$W(\cdot, t_0) = W_0, \tag{46}$$

where $Q_{\vec{X}_0} = I - P_{\vec{X}_0}$ is the complementary projection onto the decaying space $\mathcal{Y}_{\vec{X}_0}$. The estimates of Eq. 37 in (H2) show that $\|W\|_{H^1}$ decays exponentially in time until the secular term $\mathcal{S}$ grows large enough to prevent further decay. At this time, denoted t_1, the solution U is given by

$$U_1 = U(x, t_1) = \Phi_N(x, \vec{X}(t_1)) + W(x, t_1). \tag{47}$$

From Eq. 49 and (H0), we see that the time scale $\tau = \mathcal{O}(1/\|F(\Phi_n)\|_{H^1}) = \mathcal{O}(1/\epsilon^2)$ for the pulse evolution is long compared to the decay rate k guaranteed by (H2). Thus the distance from U_1 to the quasi-steady manifold $\mathcal{M}$ can be expected to be smaller than the initial distance from U_0 to the manifold. We renormalize, determining new initial conditions $\vec{X}_1, \vec{X}_2, \ldots$ with associated decaying spaces $\mathcal{Y}_{\vec{X}_1}, \mathcal{Y}_{\vec{X}_2}, \ldots$ at times $t_1, t_2, \ldots$. The pulse evolution is given by Eq. 49 on each time interval (t_i, t_{i+1}) with a jump from the end value $\vec{X}(t_{i+1}^-)$ to the intial value of the next interval, $\vec{X}_{i+1}$ which satifies

$$\|\vec{X}(t_{i+1}^-) - \vec{X}_{i+1}\| = \mathcal{O}(\epsilon^4). \tag{48}$$

We summarize our result in the theorem below. An explicit formulation of Eqn. 49 is given in Eqns. 79 and 80 for the case $N = 2$.

Theorem 1 *For an initial condition U_0 sufficiently close to the N-pulse manifold $\mathcal{M}$, the solution U of Eqn. 16 can be decomposed as in Eqn. 20, where the pulse positions $\vec{X}$ evolve according to*

$$\dot{\vec{X}} = M^{-1}\mathcal{F}, \tag{49}$$

with M the $N \times N$ matrix given in Eqn. 39 and $\mathcal{F} \in \mathbf{R}^N$ having components

$$\mathcal{F}_j = \left(F(\Phi_N(\cdot, \vec{X})), \Psi_j^\dagger(\vec{X}) \right)_2 + \mathcal{O}(\epsilon^4). \tag{50}$$

The evolution given by Eq. 49 is valid up to $\mathcal{O}(\epsilon^4)$ jumps in $\vec{X}$ at each renormalization time t_k where $1 \gg |t_{k+1} - t_k| \gg \epsilon^2$. The remainder W satisfies

$$\|W(t)\|_{H^1} \leq c \left(\|W(0)\|_{H^1} e^{-k(t-t_0)} + \epsilon^2 \right) \tag{51}$$

for some $c > 0$ with $k > 0$ as in Eqn. 37.

3.2. Analogy with Wilsonian RG

A number of authors have formalized the application of Wilsonian RG theory to perturbed differential equations, each using a slightly different notational convention for the parameterization of the slow manifold [9, 12, 26]. These studies generally share the following two ideas: 1) that the PDE dynamics should be insensitive to an arbitrarily chosen "renormalization time" (sometimes called the arbitrary time or initial time), and 2) that the fast modes can be taken at quasi steady-state. Both of these criteria are rather heuristically justified on physical grounds, but in the ODE context have been shown to be equivalent to a normal form reduction (see Ref. 10). In the PDE setting of interest here, the Wilsonian approach gives the same reduction to leading order as the rigorous result presented above. We will frame our results in the language of Ref. 12 to show this analogy explicitly.

Introducing an arbitrary renormalization time t_0 into the ansatz given by Eqn. 19 gives

$$U(x,t) = \sum_{j=1}^{N} \alpha_j \Phi_j \left(x - X_j(t_0)\right) + \epsilon^2 W(x,t;t_0), \tag{52}$$

where U is independent of t_0 and we have rescaled W by ϵ^2 for notational convenience. This decomposition is inserted into Eqn. 16 to obtain an initial-value problem for W given by

$$W_t = L_{t_0} W + G_{t_0} + \mathcal{O}(\epsilon^2), \tag{53}$$

where $G_{t_0} \equiv F(\Phi_N(\cdot, \vec{X}(t_0)))$. This formal step is analogous to the decomposition of L in Eq. 42. Analogous to the condition Eq. 41, we require the initial condition of W for this IVP to be orthogonal to the eigenspace $\mathcal{X}_{\vec{X}(t_0)}$ of L_{t_0}. We denote the projection operator onto this eigenspace of L_{t_0} by P_{t_0}, imposing

$$P_{t_0} W(x,t_0;t_0) = 0. \tag{54}$$

The interpulse dynamics are dominated by nearest-neighbor interactions; we therefore consider two pulses ($N = 2$) and, neglecting $\mathcal{O}(\epsilon^2 |W|)$ cross-terms in L_{t_0}, we obtain

$$L_{t_0} \equiv \begin{pmatrix} 0 & D_{12}(x) \\ -C_{12}(x) & -2 \end{pmatrix} \qquad \text{and} \tag{55}$$

$$G_{t_0} \equiv \begin{pmatrix} 0 \\ 1 \end{pmatrix} \left[\frac{3}{\epsilon^2} \left(\alpha_2 \phi_1^2 \phi_2 + \alpha_1 \phi_1 \phi_2^2 \right) - \Delta a_1 \alpha_1 \phi_1 - \Delta a_2 \alpha_2 \phi_2 \right], \tag{56}$$

where, in the operator L_{t_0},

$$D_{12}(x) \equiv -\frac{1}{2}\partial_x^2 - (\phi_1^2 + \phi_2^2) + \eta_-(x) \qquad \text{and} \tag{57}$$

$$C_{12}(x) \equiv -\frac{1}{2}\partial_x^2 - 3(\phi_1^2 + \phi_2^2) + \eta_+(x), \tag{58}$$

while in G_{t_0} we have introduced the spatially dependent refractive index perturbation,

$$\Delta a_j(x;t_0) = \frac{a(\epsilon x) - a(\epsilon X_j(t_0))}{\epsilon^2}. \tag{59}$$

The projections onto $\mathcal{X}_{\vec{X}}$ and $\mathcal{Y}_{\vec{X}}$ are given by

$$P_{t_0} \equiv \langle \cdot, \Psi_-^\dagger \rangle \Psi_- + \langle \cdot, \Psi_+^\dagger \rangle \Psi_+ \tag{60}$$

and $Q_{t_0} \equiv I - P_{t_0}$. We formally solve Eq. 53 for W to leading order. As $L_{t_0}, P_{t_0}, Q_{t_0}$, and G_{t_0} are independent of t, we decompose Eqn. 53 into

$$(P_{t_0}W)_t = P_{t_0}G_{t_0} + \mathcal{O}(\epsilon^2) \qquad \text{and} \tag{61}$$

$$(Q_{t_0}W)_t = L_{t_0}Q_{t_0}W + Q_{t_0}G_{t_0} + \mathcal{O}(\epsilon^2). \tag{62}$$

Using Eqn. 54, these have the formal solutions

$$P_{t_0}W = (t-t_0)P_{t_0}G_{t_0} + \mathcal{O}(\epsilon^2) \qquad \text{and} \tag{63}$$

$$Q_{t_0}W = -L_{t_0}^{-1}Q_{t_0}G_{t_0} + e^{(t-t_0)L_{t_0}}(Q_{t_0}W_0 + L_{t_0}^{-1}Q_{t_0}G_{t_0}) + \mathcal{O}(\epsilon^2), \tag{64}$$

where $W_0 = W(x, t_0; t_0)$. Recalling Eqn. 54, these sum to give

$$W = e^{(t-t_0)L_{t_0}}\left[W_0 + L_{t_0}^{-1}Q_{t_0}G_{t_0}\right] + (t-t_0)P_{t_0}G_{t_0} - L_{t_0}^{-1}Q_{t_0}G_{t_0} + \mathcal{O}(\epsilon^2). \tag{65}$$

The final step is to apply what is often called the RG equation [12] to Eqns. 19 and 20, enforcing the insensitivity of the solution to the renormalization time, t_0, and then eliminating t_0 by setting it equal to t. At leading order this amounts to demanding that

$$\frac{\partial}{\partial t_0}\left\{\sum_{j=1}^{2}\alpha_j\Phi_j\left(x - X_j(t_0)\right) + \epsilon^2 W(x,t;t_0)\right\}\Bigg|_{t_0=t} = \mathcal{O}(\epsilon^4). \tag{66}$$

The quantities W_0, L_{t_0}, P_{t_0}, Q_{t_0} and G_{t_0} depend upon t_0 only through $\vec{X}_0$, whose t_0 derivative will be shown to be $\mathcal{O}(\epsilon^2)$. The only non-negligble term in the t_0 derivative of W arises from the exponential in the first term on the right-hand side of Eqn. 65, and we arrive at the equality

$$\sum_{j=1}^{2}\alpha_j X_j\Phi_j' + \epsilon^2 P_{t_0}G_{t_0} = -\epsilon^2\left(L_{t_0}W_0 + Q_{t_0}G_{t_0}\right) + \mathcal{O}(\epsilon^4) \tag{67}$$

evaluated at $t_0 = t$. Projecting this equation on the finite-dimensional $\mathcal{X}_t$ space yields, at leading order, the system of ODEs given by Eqn. 49, which is algebraically equivalent to the condition imposed in Eqn. 49. The Wilsonian RG condition Eqn. 66, however, is an even more demanding constraint. Indeed, projecting Eqn. 67 onto the infinite-dimensional space $\mathcal{Y}_{t_0}$ we obtain the system

$$W_0 = -L_{t_0}^{-1}Q_{t_0}G_{t_0}\big|_{t_0=t} + \mathcal{O}(\epsilon^2). \tag{68}$$

In the approach of Ref. 12 this equation was taken as an extra step to cancel the "dangerous" term in Eqn. 65 suggesting fast dynamics in W. In fact it follows from Eqn. 66 and is equivalent to the rigorous evaluation of W, given by Eqn. 45, under the approximation of stationarity, i.e. $W_t = 0$, and neglecting the nonlinearity and higher order terms associated with the time-dependent evolution of the slow variables $\vec{X}$. In fact, Eqn. 68 can be regarded as the first step in a Newton iteration for $F(\Phi) = 0$ beginning with initial guess $\Phi = \Phi_N$,

$$\Phi_N^{(1)} = \Phi_N(\cdot, \vec{X}) - L_{\vec{X}}^{-1} Q_{\vec{X}} F(\Phi_N(\cdot, \vec{X})). \tag{69}$$

In the case of two pulses, substituting Eqn. 68 into Eqn. 67 gives two equations, one for each eigenfunction in the kernel of L_{t_0}, for the two free parameters in the ansatz:

$$\alpha_1 \dot{X}_1 - \alpha_2 \dot{X}_2 = -\epsilon^2 \langle G_{t_0}, \Psi_1^\dagger \rangle + \epsilon^2 \langle G_{t_0}, \Psi_2^\dagger \rangle + \mathcal{O}(\epsilon^4), \tag{70}$$

$$\alpha_1 \dot{X}_1 + \alpha_2 \dot{X}_2 = -\epsilon^2 \langle G_{t_0}, \Psi_1^\dagger \rangle - \epsilon^2 \langle G_{t_0}, \Psi_2^\dagger \rangle + \mathcal{O}(\epsilon^4). \tag{71}$$

These equations agree with Eqn. 49 up to $\mathcal{O}(\epsilon^4)$.

4. Reduced dynamics and numerics

We compare the reduced dynamics obtained from the analysis above with simulations of the full PDE for both a single pulse and two interacting pulses. In all cases except for that involving two pulses with the same sign, the error was of the same order or smaller than $\epsilon^4 t$, as predicted by Eqns. 70 and 71. The case of two pulses with identical sign is described in more detail below.

4.1. One pulse

We first briefly consider the case of a single pulse, obtained by setting $\phi_2 = 0$ in the derivation above and in Eqn. 56 for G_{t_0}. Dropping the subscripts, we are left with

$$\dot{X} = \epsilon^2 \left\langle \begin{pmatrix} 0 \\ 1 \end{pmatrix} \Delta a(x; X)\, \phi_X(x - X), \Psi_X^\dagger(x - X) \right\rangle + \mathcal{O}(\epsilon^4) \tag{72}$$

$$= -\frac{\epsilon^2}{2\Theta(X)} \int \phi_X^2(x - X) \Delta a'(x; X)\, dx + \mathcal{O}(\epsilon^4) \tag{73}$$

$$= \frac{\epsilon^2 a_1}{2\Theta(X)} \int \mu\, \mathrm{sech}^2(\mu - \sqrt{2\eta(X)} X) \exp\left(-\frac{\epsilon^2 \mu^2}{4\eta(X)} \right) d\mu + \mathcal{O}(\epsilon^4). \tag{74}$$

The evolution of $X(t)$ describes the effect of the perturbed refractive index on the motion of a single pulse. We have explicitly included the dependencies on X to show the nature of the ODE.

Linearizing about $X = 0$ (i.e., close to the center of the refractive index perturbation) picks out the linear variation in $\Delta a'(x; X)$ across the pulse, giving

exponential growth or decay depending on the sign of a_1:

$$\dot{X} = \frac{\epsilon^2 a_1}{\Theta_0}\sqrt{2\eta_0}X + \mathcal{O}(\epsilon^4 X), \tag{75}$$

where Θ_0 and η_0 are evaluated at $X = 0$. For pulses far from the center of the index perturbation, Taylor-expanding $\phi^2(x - X; X)$ about $x = 0$ or $\Delta a'(x; X)$ about $x = X$, depending on the particular limit, gives

$$\dot{X} = \frac{\epsilon^2 a_1}{\Theta_\infty}\sqrt{2\eta_\infty}X \exp\left(-\frac{1}{2}\epsilon^2 X^2\right) + \mathcal{O}\left[\epsilon^2(1+\epsilon^2 X^2)e^{-\frac{1}{2}\epsilon^2 X^2} + \epsilon^4\right] \tag{76}$$

if $|X| \ll 1/\epsilon^2$, and

$$\dot{X} = \mathrm{sgn}(X)\frac{16 a_1\sqrt{\pi}\eta_\infty^{3/2}}{\epsilon\Theta_\infty}\ \exp(4\eta_\infty/\epsilon^2 - 2\sqrt{2\eta_\infty}|X|) + \mathcal{O}\left[\frac{1}{\epsilon}\exp\left(-4\sqrt{2\eta_\infty}|X|\right)\right] \tag{77}$$

if $|X| \gg 1/\epsilon^2$. Here, $\eta_\infty = a_0 + \sqrt{\gamma^2 - 1}$ and Θ_∞ are the asymptotic values of η_+ and Θ, respectively, as $X \to \pm\infty$.

Physically, the case $a_1 < 0$ corresponds to a refractive index that is greatest in the center of the OPA. This gives rise to thermal lensing, where the optical beam is guided into the center of the OPA by the refractive index gradient. The opposite case, where $a_1 > 0$, causes the beam to deflect outwards from the center of the OPA. These behaviors are confirmed in Figs. 5 and 6, respectively.

4.2. Two pulses

In the case of two pulses, the dynamic equations are

$$\begin{aligned}\dot{X}_j =& \frac{1}{\Theta(X_j)}\left[\alpha_1\alpha_2\int \phi^3_{X_j}(x - X_j)\phi'_{X_{3-j}}(x - X_{3-j})\,dx\right.\\ &\left.-\frac{\epsilon^2}{2}\int \phi^2_{X_j}(x - X_j)\Delta a'(x; X_j)\,dx\right] + \mathcal{O}(\epsilon^4)\end{aligned} \tag{78}$$

for $j = 1, 2$. The interesting case is where the pulses are close enough to balance their mutual interaction against the influence of the external potential generated by the refractive index gradient. We write $Y_1 \equiv X_2 - X_1$ and $Y_2 \equiv X_2 + X_1$, and assume without loss of generality that $Y_1 > 0$. Some manipulation yields

$$\begin{aligned}\dot{Y}_1 =& -\frac{1}{\Theta_0}\left[8\alpha_1\alpha_2(2\eta_0)^2 e^{-\sqrt{2\eta_0}Y_1} - \sqrt{2\eta_0}\epsilon^2 a_1 Y_1\right]\\ &+ \mathcal{O}(\epsilon^2 e^{-\sqrt{2\eta_0}Y_1} + e^{-2\sqrt{2\eta_0}Y_1}) \qquad \text{and}\end{aligned} \tag{79}$$

$$\dot{Y}_2 = \frac{\epsilon^2 a_1}{\Theta_0}\sqrt{2\eta_0}Y_2 + \mathcal{O}(\epsilon^2 e^{-\sqrt{2\eta_0}Y_1} + e^{-2\sqrt{2\eta_0}Y_1}) \tag{80}$$

In Eqn. 79, one can see directly the competing influences of the perturbed refractive index, which serves as a waveguide in the OPA, and the pulse-pulse interactions. The former acts as a longer-range force relative to the exponential dependence of pulse-pulse effects on pulse separation. We readily obtain the following results:

Theorem 2 *For the two pulse ansatz, Eq. 19 with $N = 2$, there exists a stationary bound pulse pair if and only if* $\mathrm{sgn} a_1 = \alpha_1\alpha_2$. *The pulses are located symmetrically about the origin and have a pulse separation Y_s that satisfies*

$$Y_s = \frac{8\alpha_1\alpha_2}{\epsilon^2 a_1}(2\bar{\eta})^{3/2} e^{-\sqrt{2\bar{\eta}}Y_s} \tag{81}$$

at leading order. The steady two-pulse configuration is stable if and only if $\alpha_1 \neq \alpha_2$ and $a_1 < 0$.

Proof: Linearization of Eq. 79 about $Y_1 = Y_s$ yields,

$$\dot{y} = \frac{\sqrt{2\bar{\eta}}\epsilon^2 a_1}{\Theta}\left(1 + \sqrt{2\bar{\eta}}Y_s\right) y. \tag{82}$$

The equilibrium $(Y_1, Y_2) = (Y_s, 0)$ is stable if $a_1 < 0$, which from the existence condition requires $\alpha_1\alpha_2 = -1$. The PDE solution inherits stability of the ODE solution, modulo motion within an $\mathcal{O}(\epsilon^4)$ neighborhood of the fixed point $\Phi_{N=2}(\cdot, (Y_s, 0))$. Physically, the existence criteria for a unique and stable steady state correspond to the case where the pulses are oppositely signed and repel each other, but where this repulsion is arrested by thermal lensing through perturbations induced in the refractive index. That this case leads to a stable steady state is consistent with a balance between a repulsive short-range force and an attractive long-range force. The opposite case, in which the short-range inter-pulse force is attractive and the long-range thermal gradient is repulsive, can produce only an unstable steady state. Figure 7 gives an example of a stably bound pulse pair and the refractive index perturbation that produces it.

Figures 8 and 9 depict the following four cases: (i) similarly signed pulses with no index perturbation, (ii) similarly signed pulses with a positive index perturbation, (iii) oppositely signed pulses with no index perturbation and (iv) oppositely signed pulses with a negative index perturbation. As predicted by the analysis above, only cases (ii) and (iii) allow for steady states, and this steady state is only stable in the latter case. As stated above, the agreement between the PDE numerics and the ODE numerics is within $\mathcal{O}(\epsilon^4 t)$ in all cases except for the two in-phase pulses. The poor agreement in this case is due to the dynamics of the problem, in that similar initial conditions near the unstable fixed point diverge exponentially, ultimately leading to $\mathcal{O}(1)$ differences in timing. Furthermore, as the pulses coalesce, the spectrum deviates significantly from the perturbative description, eventually violating (H1) and rendering the ODEs invalid.

5. Conclusions

We have presented a rigorous reduction for the dynamics of pulse pairs in the perturbed PNLS equation, obtaining a two-dimensional system of ODEs for the pulse positions. We have compared this rigorous derivation with the formal Wilsonian RG approach, finding that the two predict identical leading order dynamics. However the rigorous construction indicates key steps essential for the accuracy of the reduced system. Chief

among these is a form of normal hyperbolicity (H1), in the sense that the spectrum of the linearized operator must be resolvable into an "active" part consisting of a finite number of eigenvalues clustered around the origin, and a damped part consisting of continuous spectrum and the remaining discrete spectrum well-separated from the active part and to the left of the imaginary axis. Another important requirement is that the tangent plane to the manifold described by the ansatz be compatible with the active part of the linearized spectrum, see (H3).

Using this construction, we have studied the evolution of single pulses and the interaction of two pulses in the presence of a Gaussian refractive index profile, with application to self-heated OPOs. We have focused on the case $\gamma - 1 = \mathcal{O}(1)$ to determine how the pulses move through interaction and perturbation; for values of γ closer to one, the second eigenfunction associated with λ_p must also be considered, producing a four-dimensional system of ODEs. This discussion is left for future work, as is the extension to coupling the optical fields back to the thermal gradients via a heat equation with a driving term dependent on the electric field intensity.

Acknowledgments

The first author acknowledges support from the Natural Sciences and Engineering Research Council of Canada. The second author acknowledges support from the National Science Foundation under grant DMS 0345705. Both authors thank Björn Sandstede and Arnd Scheel for helpful discussions concerning Ref. 23.

References

[1] N. V. Alexeeva, I. V. Barashenkov, and D. E. Pelinovsky. Dynamics of the parametrically driven NLS solitons beyond the onset of the oscillatory instability. *Nonlinearity*, 12:103–140, 1999.

[2] G. Arisholm, E. Lippert, G. Rustad, and K. Stenersen. Efficient conversion from 1 to 2 μm by a KTP-based ring optical parametric oscillator. *Opt. Lett.*, 27(15):1336–1338, August 2002.

[3] I. V. Barashenkov, M. M. Bogdan, and V. I. Korobov. Stability diagram of the phase-locked solitons in the parametrically driven, damped nonlinear Schrödinger equation. *Europhys. Lett.*, 15(2):113–118, May 1991.

[4] I. V. Barashenkov and E. V. Zemlyanaya. Traveling solitons in the damped-driven nonlinear Schrödinger equation. *SIAM J. Appl. Math.*, 64(3):800–818, 2004.

[5] I. V. Barashenkov, E. V. Zemlyanaya, and M. Bär. Traveling solitons in the parametrically driven nonlinear Schrödinger equation. *Phys. Rev. E*, 64:016603, 2001.

[6] I. Barashenkov and E. Zamlyanaya. Stable complexes of parametrically driven, damped nonlinear Schrödinger solitons. *Phys. Rev. Lett.*, 83:2568–2571, 1999.

[7] P. A. C.-Y. Chang. *Modulational stability of oscillatory pulse solutions of the parametrically forced nonlinear Schrödinger equation.* PhD thesis, Simon Fraser University, December 2003.

[8] L. Y. Chen, N. Goldenfeld, and Y. Oono. Renormalization-group theory and variational calculations for propagating fronts. *Phys. Rev. E*, 49(5):4502–4511, May 1994.

[9] L. Y. Chen, N. Goldenfeld, and Y. Oono. Renormalization group and singular perturbations: Multiple scales, boundary layers, and reductive perturbation theory. *Phys. Rev. E*, 54(1):376–394, July 1996.

[10] R. E. Deville, A. Harkin, K. Josic, and T. J. Kaper. Applications of asymptotic normal form theory and its connections with a renormalization group method. *submitted Feb. 2004*.

[11] M. Ebrahinzadeh. Parametric light generation. *Phil. Trans. Roy. Soc. London A*, 361(1813):2731–2750, December 2003.

[12] S. I. Ei, K. Fujii, and T. Kunihiro. Renormalization-group method for reduction of evolution equations; invariant manifolds and envelopes. *Ann. Phys.*, 280(2):236–298, March 2000.

[13] D. Henry. *Geometric theory of semilinear parabolic equations*, volume 840 of *Lecture Notes in Mathematics*. Springer-Verlag, New York, 1981.

[14] D. H. Jundt. Temperature-dependent Sellmeier equation for the index of refraction, $n(e)$, in congruent lithium niobate. *Opt. Lett.*, 22(20):1553–1555, October 1997.

[15] T. Kapitula and B. Sandstede. Stability of bright solitary-wave solutions to perturbed nonlinear Schrödinger equations. *Physica D*, 124(1-3):58, December 1998.

[16] T. J. Kulp, S. E. Bisson, R. P. Bambha, T. A. Reichardt, U. B. Goers, K. W. Aniolek, D. A. V. Kliner, B. A. Richman, K. M. Armstrong, R. Sommers, R. Schmitt, P. E. Powers, O. Levi, T. Pinguet, M. Fejer, J. P. Koplow, L. Goldberg, and T. G. McRae. The application of quasi-phase-matched parametric light sources to practical infrared chemical sensing systems. *Appl. Phys. B*, 75(2-3):317–327, September 2002.

[17] R. O. Moore. *A Study of Optical Devices with Parametric Gain*. PhD thesis, Northwestern University, Engineering Sciences and Applied Mathematics, 2001.

[18] R. O. Moore, G. Biondini, and W. L. Kath. Self-induced thermal effects and modal competition in continuous-wave optical parametric oscillators. *J. Opt. Soc. Am. B*, 19(4):802–811, April 2002.

[19] K. Promislow. A renormalization method for modulational stability of quasi-steady patterns in dispersive systems. *SIAM J. Anal. Math. Anal.*, 33(6):1455–1482, August 2002.

[20] K. Promislow and J. N. Kutz. Bifurcation and asymptotic stability in the large detuning limit of the optical parametric oscillator. *Nonlinearity*, 13(3):675–698, May 2000.

[21] A. Sanchez and A. R. Bishop. Collective coordinates and length-scale competition in spatially inhomogeneous soliton-bearing equations. *SIAM Rev.*, 40(3):579–615, 1998.

[22] B. Sandstede. Stability of multiple-pulse solutions. *Trans. Amer. Math. Soc.*, 350(2):429–472, February 1998.

[23] B. Sandstede and A. Scheel. Defects in oscillatory media: Toward a classification. *SIAM J. Appl. Dyn. Sys.*, 3(1):1–68, 2004.

[24] J. M. Song, R. Jagannathan, D. L. Stokes, P. M. Kasili, M. Panjehpour, M. N. Phan, B. F. Overholt, R. C. DeNovo, X. G. Pan, R. J. Lee, and V. D. Tuan. Development of a fluorescence detection system using optical parametric oscillator (OPO) laser excitation for in vivo diagnosis. *Tech. Cancer Res. Treat.*, 2(6):515–523, December 2003.

[25] M. M. J. W. van Herpen, S. E. Bisson, and F. J. M. Harren. Continuous-wave operation of a single-frequency optical parametric oscillator at 4-5 μm based on periodically poled LiNbO3. *Opt. Lett.*, 28(24):2497–2499, December 2003.

[26] M. Ziane. On a certain renormalization group method. *J. Math. Phys.*, 41(5):3290–3299, May 2000.

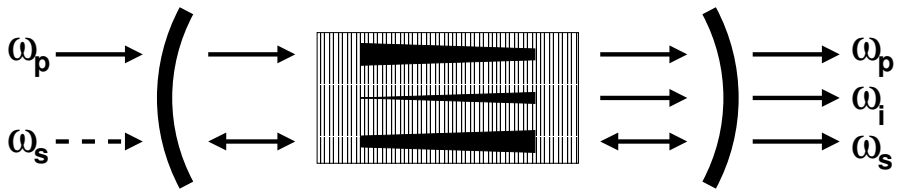

Figure 1. Schematic of an OPO consisting of a quadratically nonlinear crystal in a linear cavity. The arrows labeled ω_p, ω_s and ω_i represent pump, signal and idler fields, respectively.

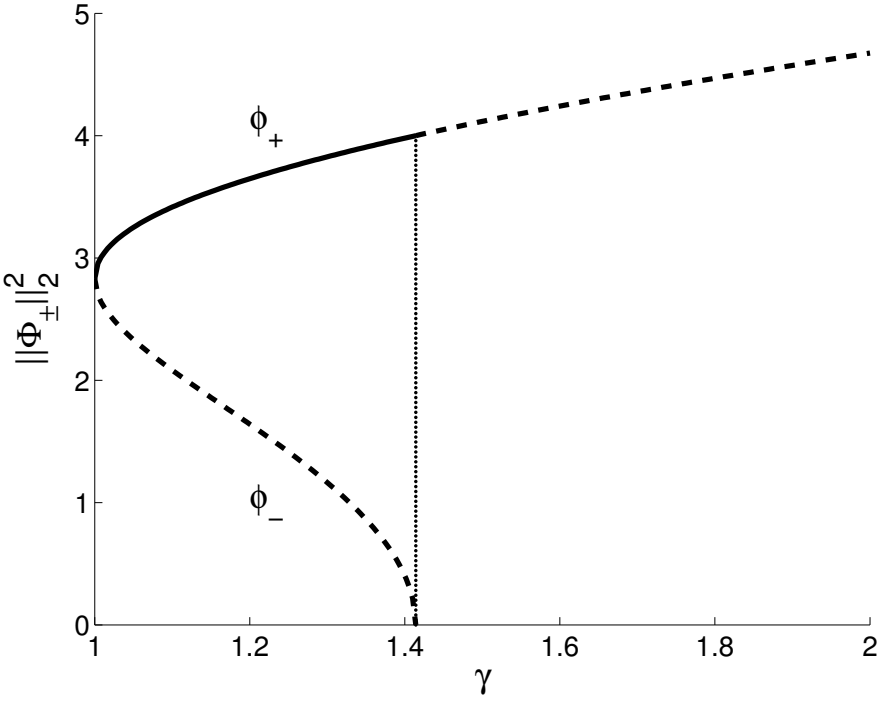

Figure 2. Bifurcation diagram of PNLS solitons for $a = 1$. Solid lines denote stable solution curves and dashed lines denote unstable solution curves. The upper branch goes unstable via an essential instability at $\gamma = \sqrt{1 + a^2}$, the same point at which the lower branch vanishes (as illustrated by the long-dashed line).

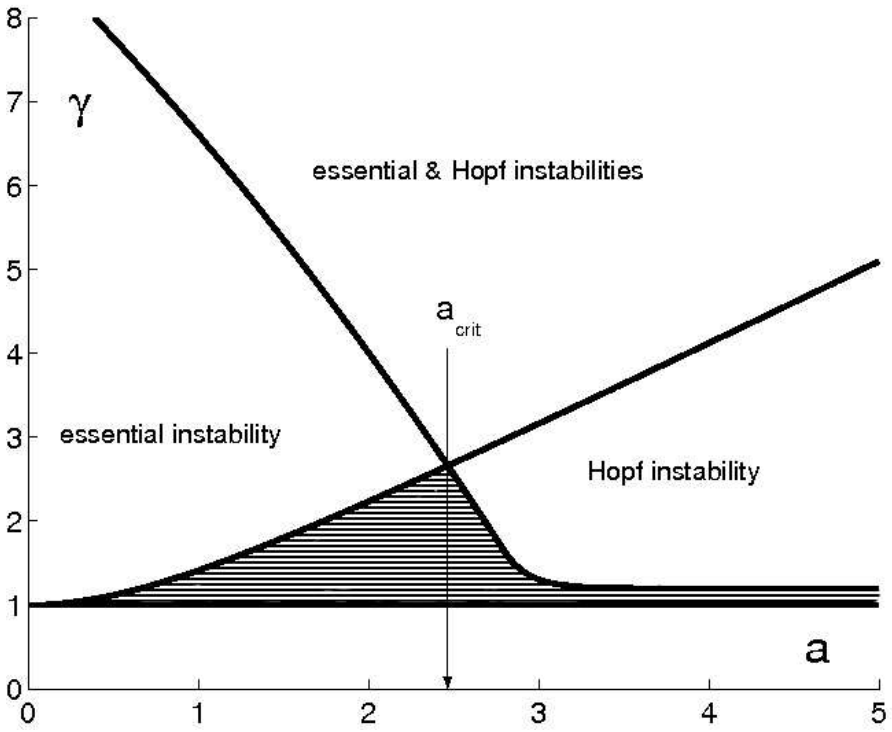

Figure 3. Stability diagram for the upper branch of PNLS solitons with constant a. Existence of the soliton requires that $\gamma \geq 1$. For $a \leq a_{\rm crit}$, the soliton undergoes an essential instability as γ increases past $\sqrt{1+a^2}$. For $a > a_{\rm crit}$, the soliton first undergoes a Hopf bifurcation (referred to in Ref. 3 as a "local mode" instability) before encountering the essential instability. The analysis given here applies only within the patterned region.

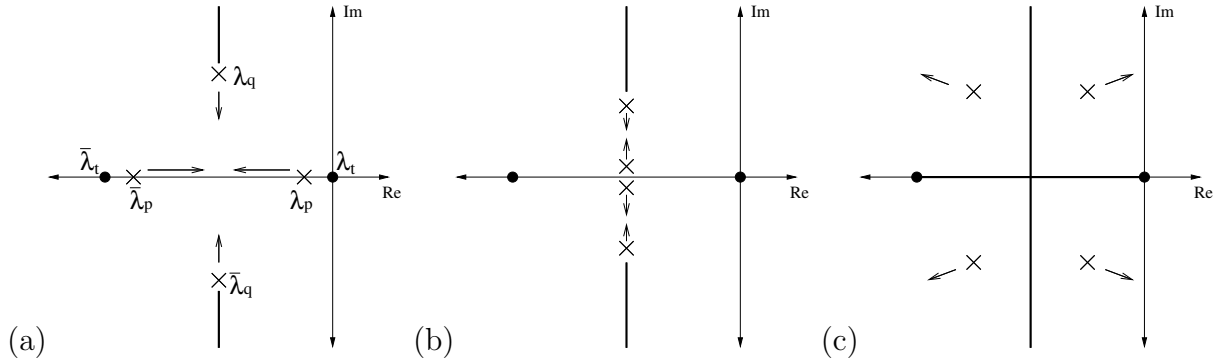

Figure 4. Linearized spectrum about the upper branch for $1.132 < a < a_{\rm crit}$ (i.e., a is large enough to have the moving eigenvalues collide on the symmetry abscissa, but small enough to have the essential instability occur before the Hopf bifurcation). Filled circles represent the pinned eigenvalues corresponding to symmetries in the PNLS equation, $\times$'s correspond to eigenvalues that depend on a and γ, and the thick line represents the essential spectrum. The figures represent the following cases for γ (where $\gamma_1 < \gamma_2 < \sqrt{1+a^2}$): (a) $1 < \gamma < \gamma_1$; (b) $\gamma_1 < \gamma < \gamma_2$; (c) $\gamma = \sqrt{1+a^2}$.

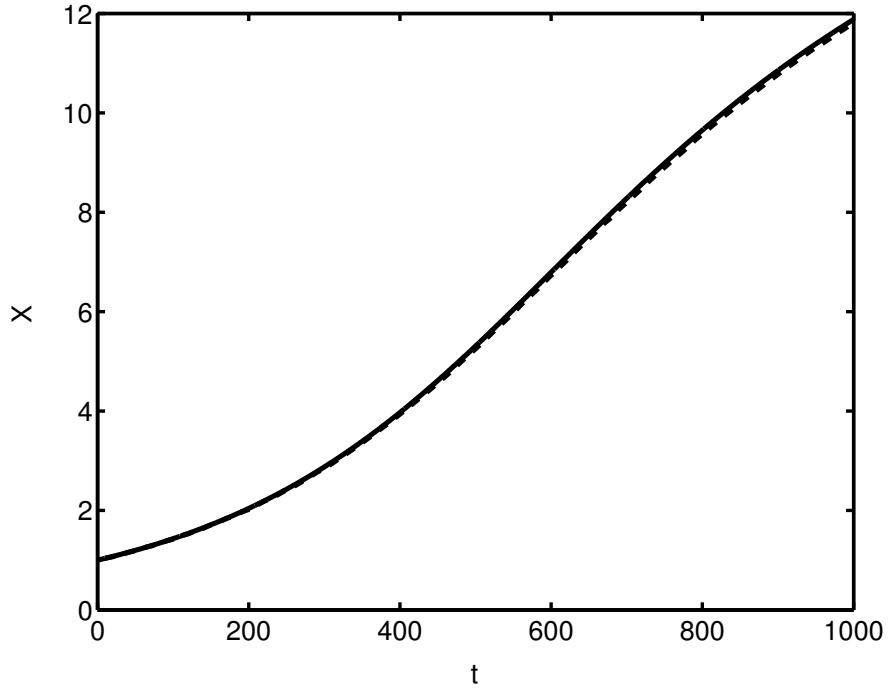

Figure 5. Comparison between ODE (solid line) and PDE numerics (dashed line) for a single pulse, at $\gamma = 1.2$, $a_0 = 0.8$, $a_1 = 0.9$ and $\epsilon = 0.125$.

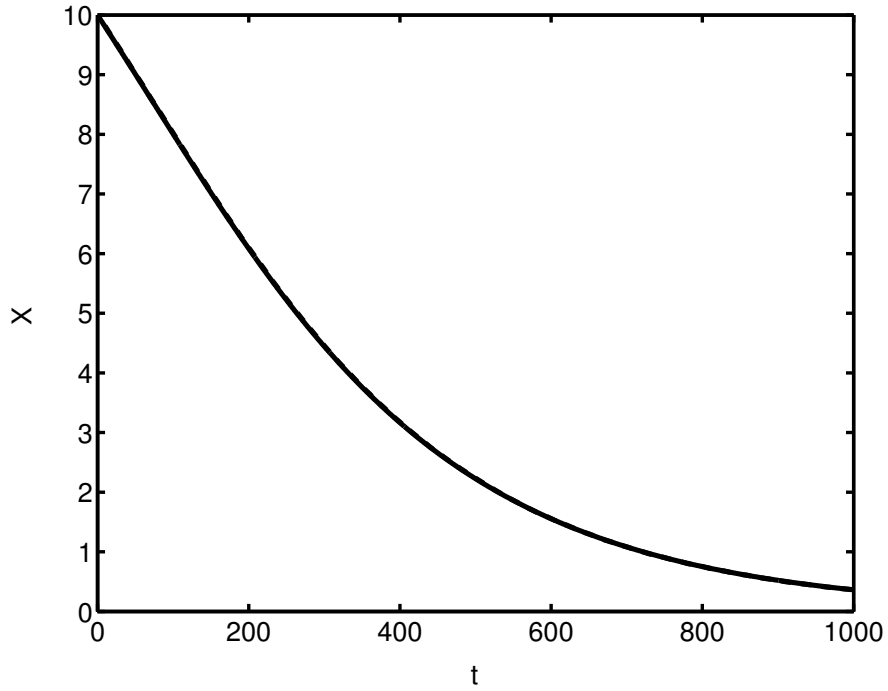

Figure 6. Comparison between ODE (solid line) and PDE numerics (dashed line) for a single pulse, at $\gamma = 1.2$, $a_0 = 2.6$, $a_1 = -0.9$ and $\epsilon = 0.125$.

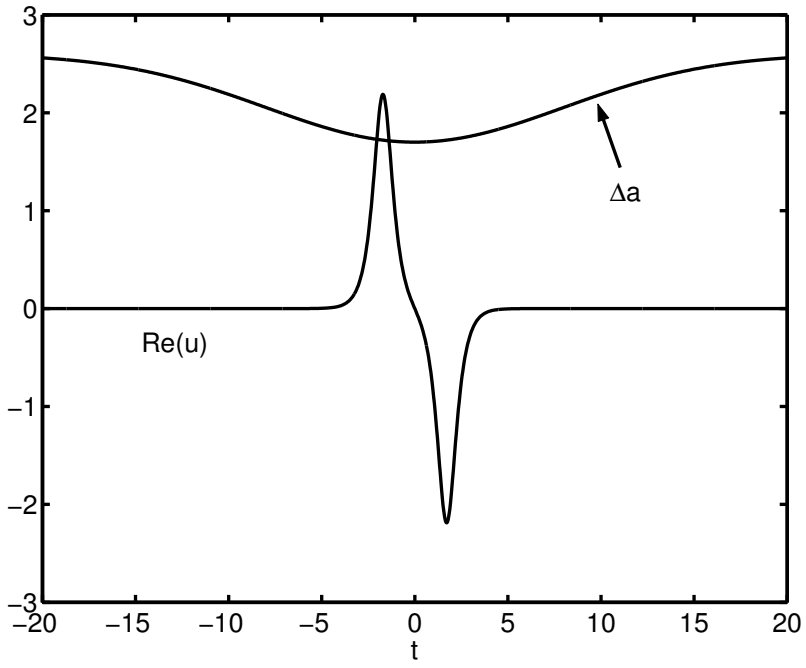

Figure 7. Stably bound pulse pair produced by inserting oppositely signed quasi-steady states into a medium with a positive refractive index perturbation ($\Delta a < 0$).

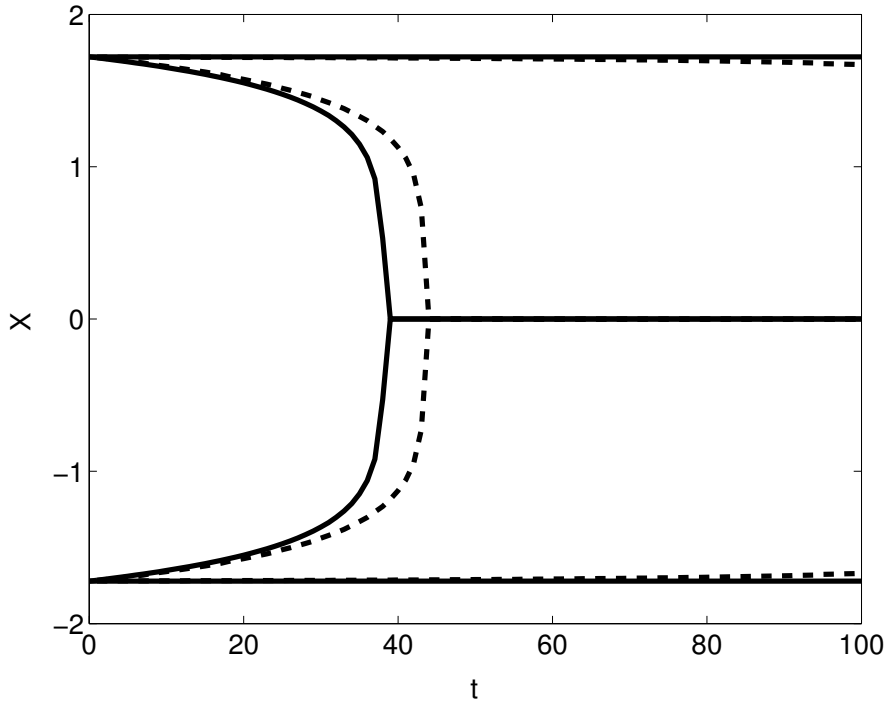

Figure 8. Two pulses with the same sign, first with a uniform ($a_0 = 1.7$ and $a_1 = 0.0$) and then brought to an *unstable* equilibrium by a positive Gaussian ($a_0 = 0.8$ and $a_1 = 0.9$). The other parameters are $\gamma = 1.2$ and $\epsilon = 0.125$. The solid curve represents ODE numerics and the dashed curve represents PDE numerics.

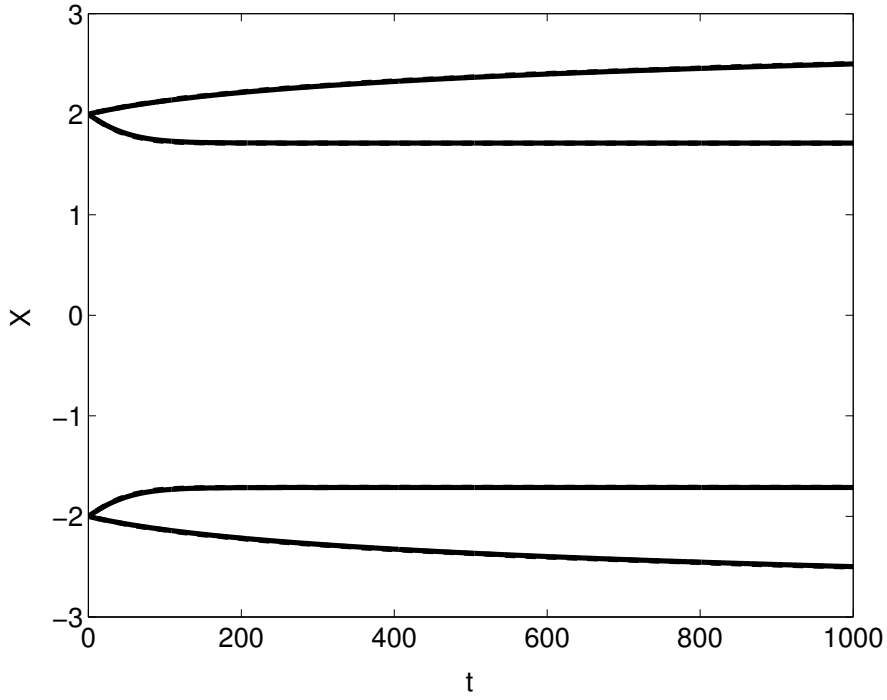

Figure 9. Two pulses with opposite signs, first with a uniform (as in Fig. 8) and then brought to a *stable* equilibrium by a negative Gaussian ($a_0 = 2.6$ and $a_1 = -0.9$). The other parameters are $\gamma = 1.2$ and $\epsilon = 0.125$. The ODE numerics and PDE numerics are indistinguishable.